Star Formation Newsletter #358 15-28

武藤恭之

No. 16

Searching for H_α-emitting sources in the gaps of five transitional disks. SPHERE/ZIMPOL high-contrast imaging

N. Huélamo, G. Chauvin, I. Mendigutía, E. Whelan, J. M. Alcalá, G. Cugno, H. M. Schmid, I. de Gregorio-Monsalvo, A. Zurlo, D. Barrado, M. Benisty, S. P. Quanz, H. Bouy, B. Montesinos, Y. Beletsky, J. Szulagyi ★

(Pre-)transitional disks show gaps and cavities that can be related with on-going planet formation. According to theory, young embedded planets can accrete material from the circumplanetary and circumstellar disks, so that they could be detected in accretion tracers, like the H_α emission line. In this work, we present spectral angular differential imaging AO-assisted observations of five (pre-)transitional disks obtained with SPHERE/ZIMPOL at the Very Large Telescope (VLT). They were obtained in the H_α line and the adjacent continuum. We have combined spectral and angular differential imaging techniques to increase the contrast in the innermost regions close to the star, and search for the signature of young accreting protoplanets. As a result, the reduced images do not show any clear H_α point source around any of the targets. We report faint H_α emissions around TW Hya and HD163296: while the former is most probably an artifact related with a spike, the nature of the latter remains unclear. The spectral and angular differential images yield contrasts of 6–8 magnitudes at separations of $\sim$ 100 mas from the central stars, except in the case of LkCa15, with values of $\sim$3 mag. We have estimated upper limits to the accretion luminosity of potential protoplanets, obtaining that planetary models provide an average value of $L_{\rm acc} \sim 10^{-4}\ L_\odot$ at 200 mas, which is $\sim$2 orders of magnitude higher than the $L_{\rm acc}$ estimated from the extrapolation of the L_{H_α} - L_{acc} stellar relationship. We explain the lack of protoplanet detections as a combination of different factors, like e.g. episodic accretion, extinction from the circumstellar and circumplanetray disks, and/or a majority of low-mass, low-accreting planets.

- 遷移円盤 5 天体の穴の中に、Ha 放射があるかを SPHERE/ZIMPOL を用いて調べる
  - RXJ1615, LkCa 15, TW Hya, T Cha, HD163296
- TW Hya と HD163296 に、弱い点源らしきものを見つけた
  - TW Hya については、スペックルの可能性が高い。過去の candidate の位置には無い
  - HD163296 については、本物の点源かもしれないが、過去の candidate の位置には無い

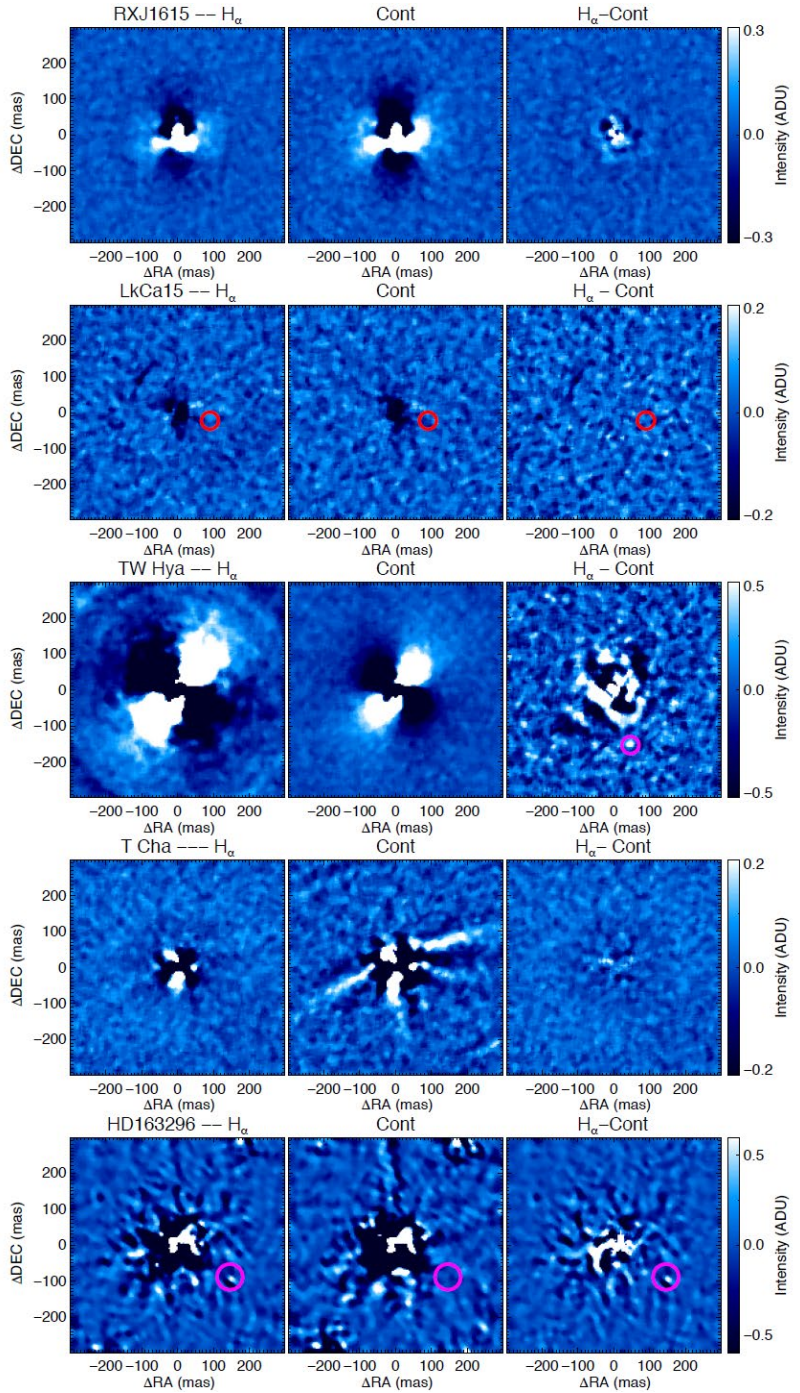

SPHERE/ZIMPOL による高コントラスト撮像
ADI と SDI を用いて解析（ASDI）

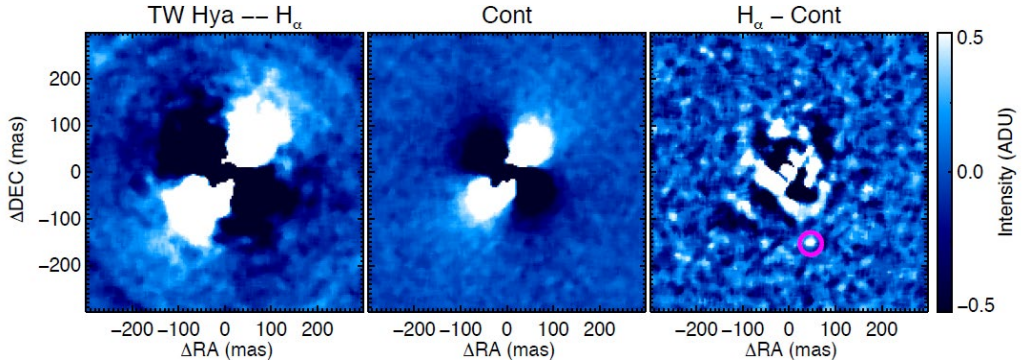

他にもいくつかの手法を用いて解析
TW Hya の例：

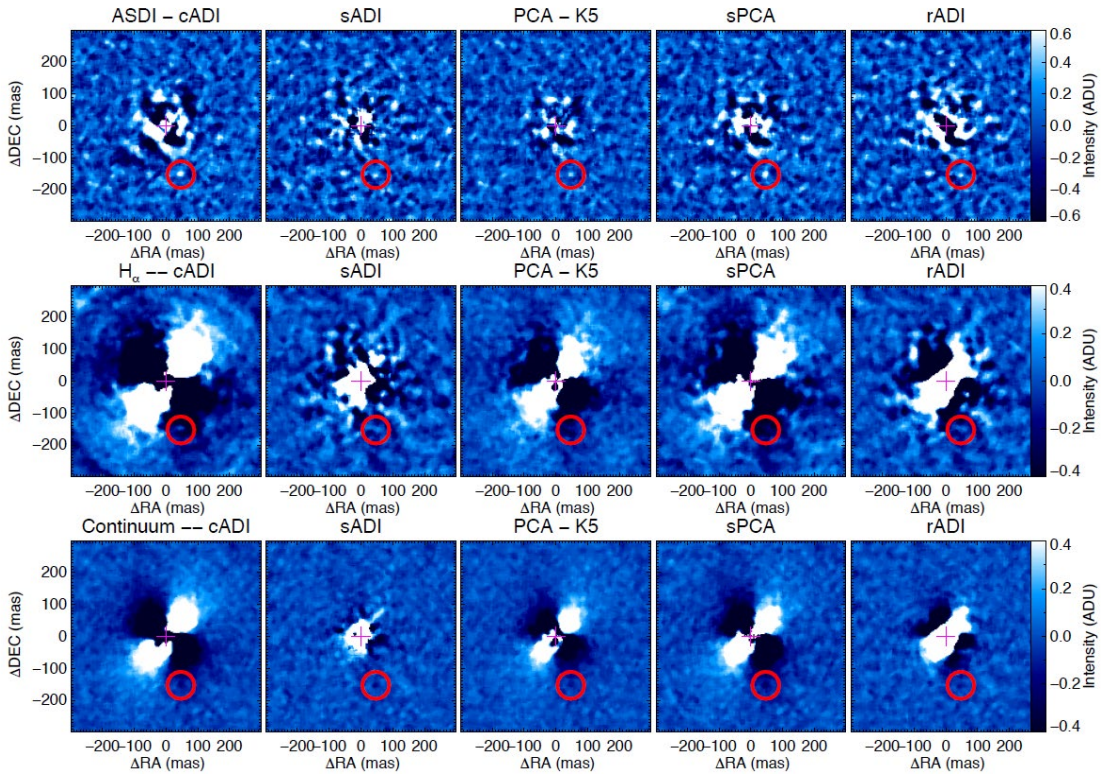

HD163296：
- 南西方向、中心星から 171mas 離れた場所に何かある
- ただし、天頂近くに来るターゲットのため、ADI がよく回らない

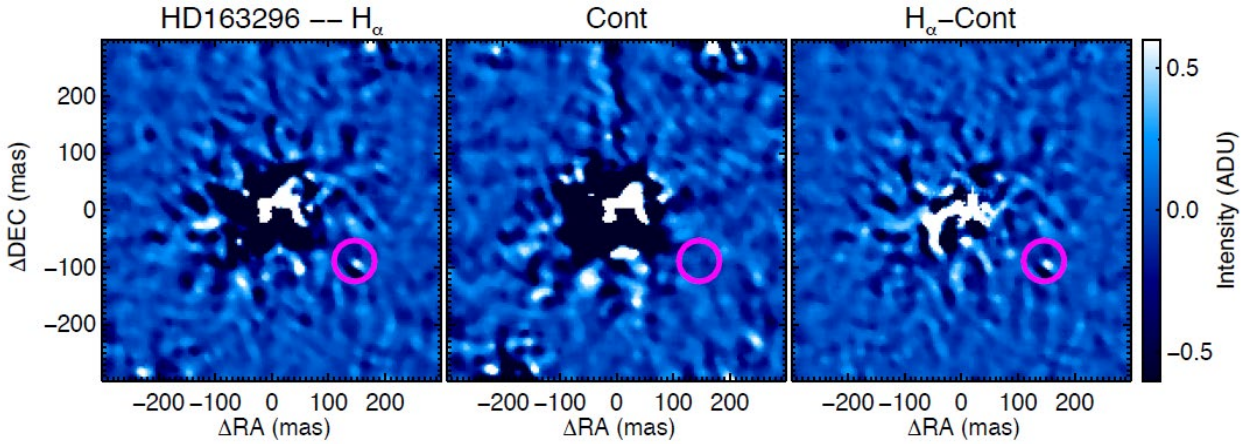

どのターゲットでも、ダストギャップの位置に Ha は見つからなかった

Target	Projected Separation (arcsec)	(au)*	Planet mass (M_{Jup})	N_Ha contrast (mag)	$F_{H\alpha}$ (10^{-15} erg/s/cm^2)	$L_{H\alpha}$ (10^{-6} $L_\odot$)	$logL_{acc}$ † ($L_\odot$)
RXJ1615	0.14[1,(g)]	22	4.5[1]	8.1	< 1.3	< 0.98	< -4.1
	0.50[2,(g)]	78	0.2[3]	8.6	< 0.8	< 0.64	< -4.3
LkCa 15	0.093[4,(p)]	15	6[5]	2.7	< 190	< 150	<-2.0
	0.27[6,(g)]	43	0.5[3]	4.4	< 38	< 0.29	< -2.7
TW Hya	0.10[7,(g)]	6	0.04[1]	8.2	< 14	< 1.6	< -3.9
	0.37[7,(g)]	22	0.15[3]	10.6	< 1.7	< 0.19	< -4.8
	0.87[8,(p)]	52	0.05[8]	11.1	< 1.0	<0.11	< -5.0
T Cha	0.093[9,(g)]	9	1.2[9]	6.0	< 1.6	< 0.52	< -4.4
HD 163296	0.10[10,(g)]	10		5.4	< 700	< 220	< -1.9
	0.44[11,(g)]	45		9.5	< 16	< 5.2	< -3.4
	0.5[12,(p)]	51	6[12]	9.9	< 10	< 3.3	< -3.6
	0.67[13,(p)]	68	1[13]	10.6	< 5.6	< 1.8	< -3.8
	0.77[14,(p)]	78	1[14]	10.8	< 4.5	< 1.4	< -3.9

ADI をしない解析を、異なる時期の観測で別々に適用しても、同じ場所に見える

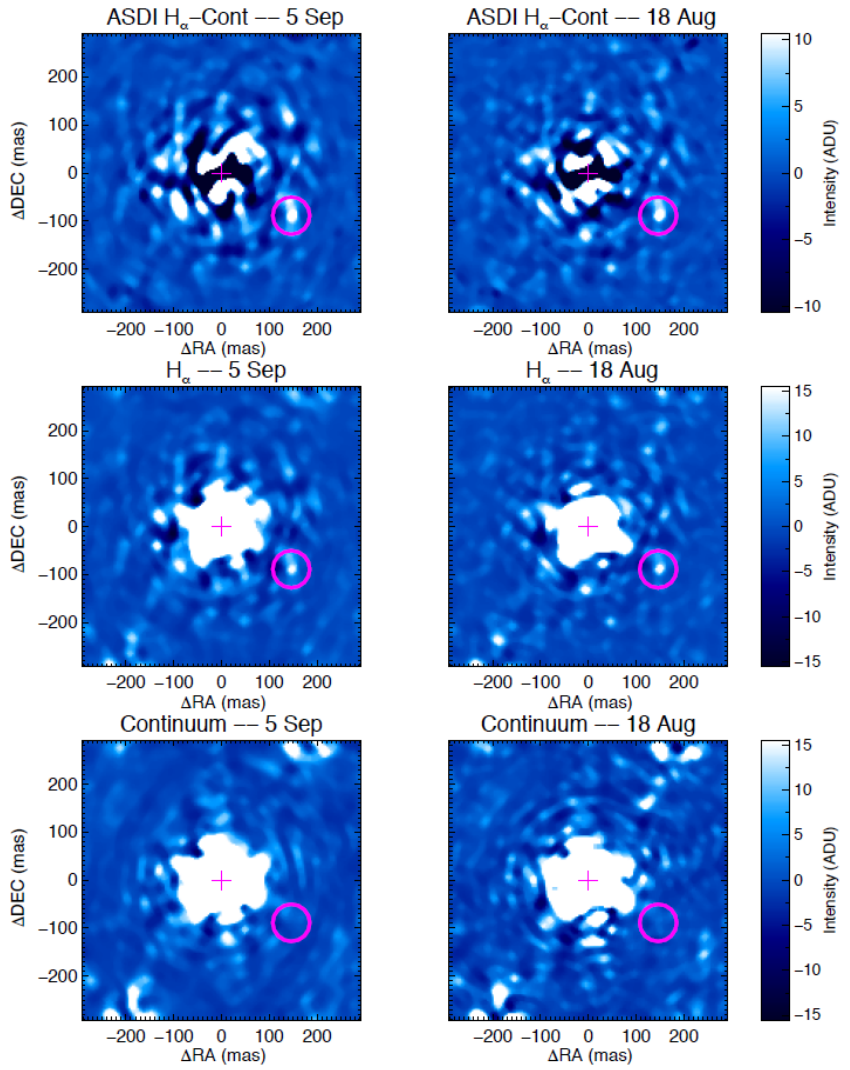

No. 20

How magnetic field and stellar radiative feedback influences the collapse and the stellar mass spectrum of a massive star forming clump

Patrick Hennebelle, Ugo Lebreuilly, Tine Colman, Davide Elia, Gary Fuller, Silvia Leurini, Thomas Nony, Eugenio Schisano, Juan D. Soler, Alessio Traficante, Ralf S. Klessen, Sergio Molinari, Leonardo Testi ★
In spite of decades of theoretical efforts, the physical origin of the stellar initial mass function (IMF) is still debated. We aim at understanding the influence of various physical processes such as radiative stellar feedback, magnetic field and non-ideal magneto-hydrodynamics on the IMF. We present a series of numerical simulations of collapsing 1000 $M_\odot$ clumps taking into account radiative feedback and magnetic field with spatial resolution down to 1 AU. Both ideal and non-ideal MHD runs are performed and various radiative feedback efficiencies are considered. We also develop analytical models that we confront to the numerical results. The sum of the luminosities produced by the stars in the calculations is computed and it compares well with the bolometric luminosities reported in observations of massive star forming clumps. The temperatures, velocities and densities are also found to be in good agreement with recent observations. The stellar mass spectrum inferred for the simulations is, generally speaking, not strictly universal and in particular varies with magnetic intensity. It is also influenced by the choice of the radiative feedback efficiency. In all simulations, a sharp drop in the stellar distribution is found at about $M_{min} \simeq 0.1$ $M_\odot$, which is likely a consequence of the adiabatic behaviour induced by dust opacities at high densities. As a consequence, when the combination of magnetic and thermal support is not too large, the mass distribution presents a peak located at 0.3-0.5 $M_\odot$. When magnetic and thermal support are large, the mass distribution is better described by a plateau, i.e. $dN/d\log M \propto M^{-\Gamma}$, $\Gamma \simeq 0$. Abridged

- 質量 1000太陽質量、半径 0.4pc のクランプにおける星形成の数値シミュレーション
- 初期磁場の強さと、星からのフィードバックが、初期質量関数にどのような影響を与えるかを議論
- 磁場の強さや星からのフィードバックは、できる星の数を減らすが、より大きな質量の星を作ることができる

基礎方程式は輻射MHD方程式、一つだけ ambipolar diffusion 入り
AMR で解く、最も良い分解能は 1.15AU
初期条件は、1000Msun のクランプが、0.4pc 程度に広がった状態
局所的な粒子数密度が 10^{13} を超えたら、sink になる

Name	R_c (pc)	μ	$\mathcal{M}$	$lmax$	dx (AU)	$f_{\rm acc}$	NMHD
NMHD10f05	0.4	10	7	18	1.15	0.5	yes
MHD10f05	0.4	10	7	18	1.15	0.5	no
MHD10f01	0.4	10	7	18	1.15	0.1	no
MHD100f05	0.4	100	7	18	1.15	0.5	no
HYDROf05	0.4	∞	7	18	1.15	0.5	no
HYDROf01	0.4	∞	7	18	1.15	0.1	no

磁場の大小　　星のフィードバック

μ: mass-to-flux ratio

facc: 星の降着エネルギーのうち、光っている割合

$$L_{\rm acc} = \frac{f_{\rm acc} G M_* \dot{M}}{R_*}$$

各 run の spapshot

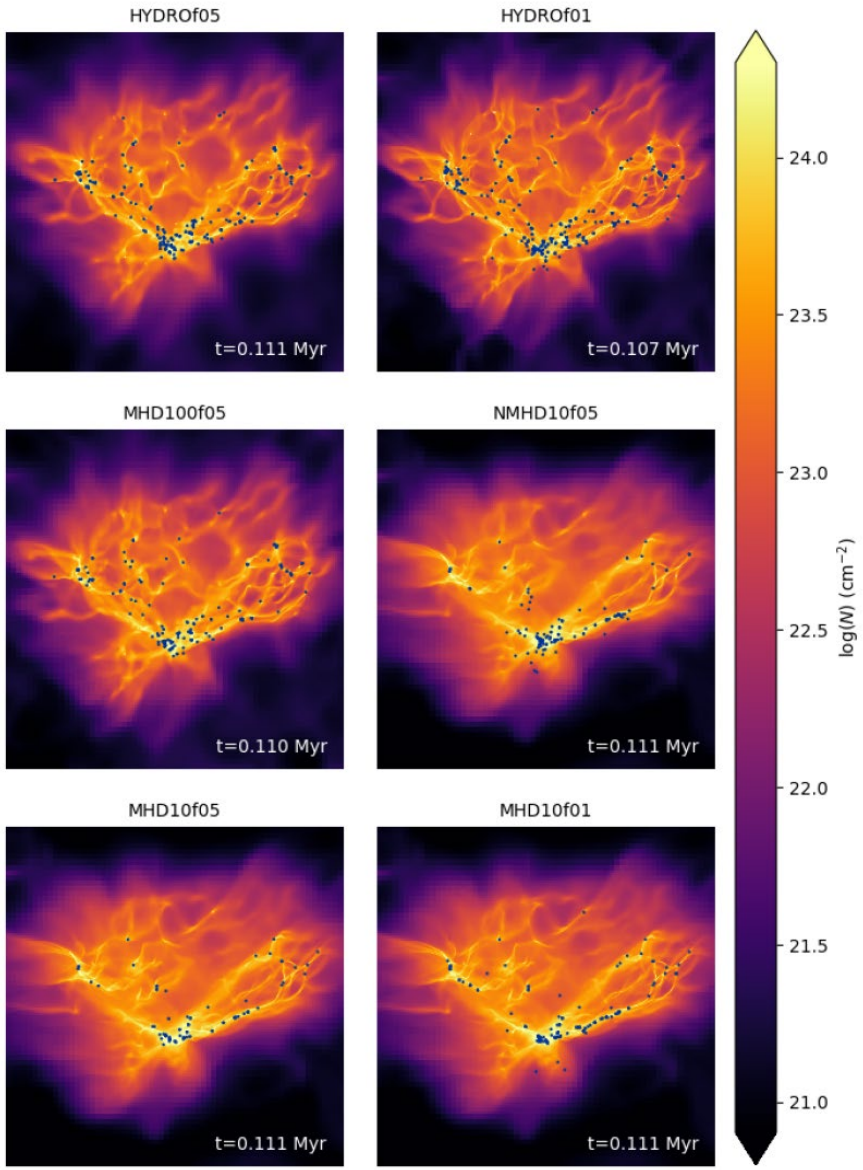

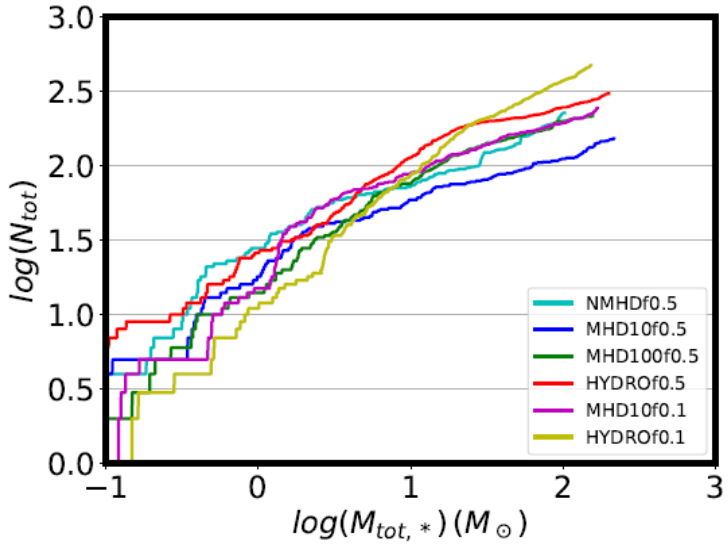

Sink 粒子の数

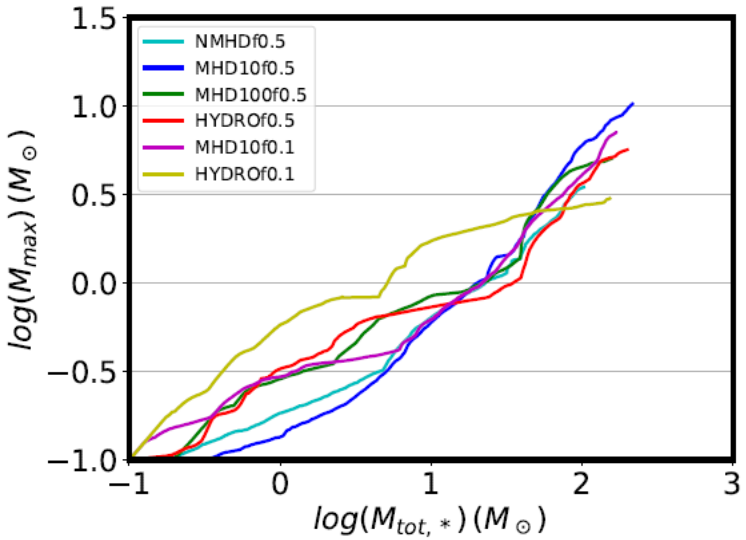

星の最大質量

磁場があると粒子数は減り、最大質量は増える

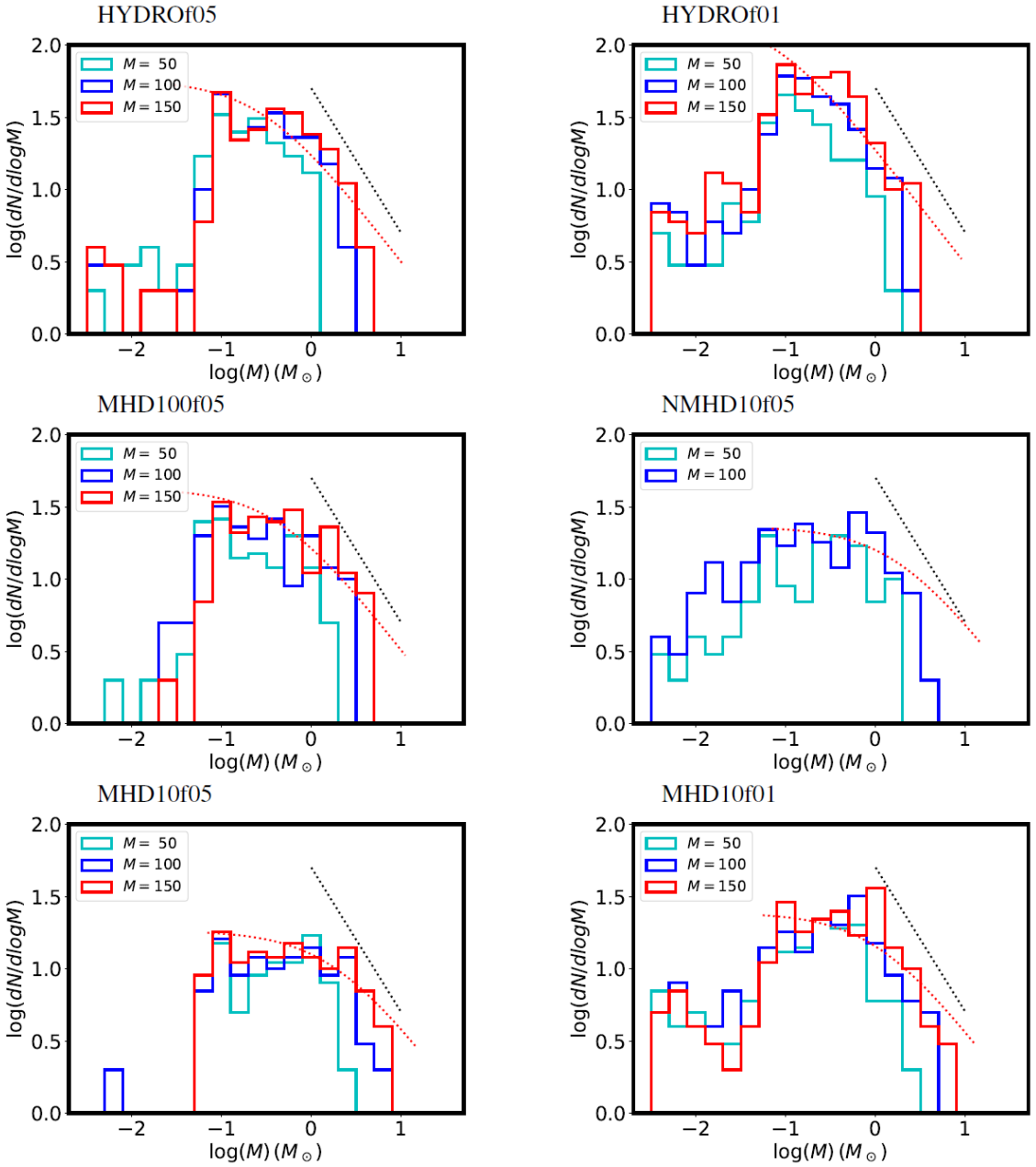

初期質量関数は：
- 基本的なべきの性質は同じ
- 磁場やフィードバックが強いと、より広がった形になる

非理想MHD

Hydro かつ フィードバック小
- 最大質量は 3Msun 程度

MHD やフィードバック大
- 星の最大質量は 7-8Msun

非理想 MHD の効果は
- 最大質量が小さい
- low-mass 側の振る舞いは解明できていない

No. 21

The Exoplanet Radius Valley from Gas-driven Planet Migration and Breaking of Resonant Chains

Andre Izidoro, Hilke E. Schlichting, Andrea Isella, Rajdeep Dasgupta, Christian Zimmermann, Bertram Bitsch

★ The size frequency distribution of exoplanet radii between 1 and $4R_\oplus$ is bimodal with peaks at $\sim$1.4 $R_\oplus$ and $\sim$2.4 $R_\oplus$, and a valley at $\sim 1.8R_\oplus$. This radius valley separates two classes of planets – usually referred to as "super-Earths" and "mini-Neptunes" – and its origin remains debated. One model proposes that super-Earths are the outcome of photo-evaporation or core-powered mass-loss stripping the primordial atmospheres of the mini-Neptunes. A contrasting model interprets the radius valley as a dichotomy in the bulk compositions, where super-Earths are rocky planets and mini-Neptunes are water-ice rich worlds. In this work, we test whether the migration model is consistent with the radius valley and how it distinguishes these views. In the migration model, planets migrate towards the disk inner edge forming a chain of planets locked in resonant configurations. After the gas disk dispersal, orbital instabilities "break the chains" and promote late collisions. This model broadly matches the period-ratio and planet-multiplicity distributions of Kepler planets, and accounts for resonant chains such as TRAPPIST-1, Kepler-223, and TOI-178. Here, by combining the outcome of planet formation simulations with compositional mass-radius relationships, and assuming complete loss of primordial H-rich atmospheres in late giant-impacts, we show that the migration model accounts for the exoplanet radius valley and the intra-system uniformity ("peas-in-a-pod") of Kepler planets. Our results suggest that planets with sizes of $\sim$1.4 $R_\oplus$ are mostly rocky, whereas those with sizes of $\sim$2.4 $R_\oplus$ are mostly water-ice rich worlds. Our results do not support an exclusively rocky composition for the cores of mini-Neptunes.

- 系外惑星の radius valley の起源について
  - 半径 ~1.4RE くらいの惑星と ~2.4RE くらいの惑星が多く、~1.8RE くらいの惑星が少ない
- Migration model で、radius valley を説明できるかを議論
  - ガス円盤中を移動してきた惑星が、resonant chain を作り、ガス散逸後に軌道が不安定化
- Migration model は、（初期条件をうまく選ぶと？）系外惑星の period ratio と multiplicity を良く説明できる
- 半径~1.4RE の惑星は岩石惑星、~2.4RE の惑星は氷惑星であることが示唆され、mini-Neptune のコアには岩石があまり多くない

モデル：
- ガス円盤中にペブルをばらまいた状態からスタート
- ガス円盤を進化させながら、N体計算をしつつ、ペブルの成長や composition を計算
- ガス散逸後に軌道不安定が起こると、giant impact が起こる

- Model-III with $w = 0.2 - 2$ au, $t_{\rm start}$= 0.5 Myr, $R_{\rm peb}$=1 cm, and $S_{\rm peb}$=5, thereafter referred as model A;
- Model-II with $w = 0.7 - 20$ au, $t_{\rm start}$= 3 Myr, $R_{\rm peb}$=1 mm, $S_{\rm peb}$=5, thereafter referred as Model B;
- Model-III with $w = 0.2 - 2$ au, $t_{\rm start}$= 0.5 Myr, $R_{\rm peb}$=1 mm, and $S_{\rm peb}$=10; thereafter referred as model C.

➔ Rocky planets を作るモデル

➔ water-rich planets を作るモデル

➔ 両方を作るモデル

３つめのモデルでは、radius valley のような分布を再現

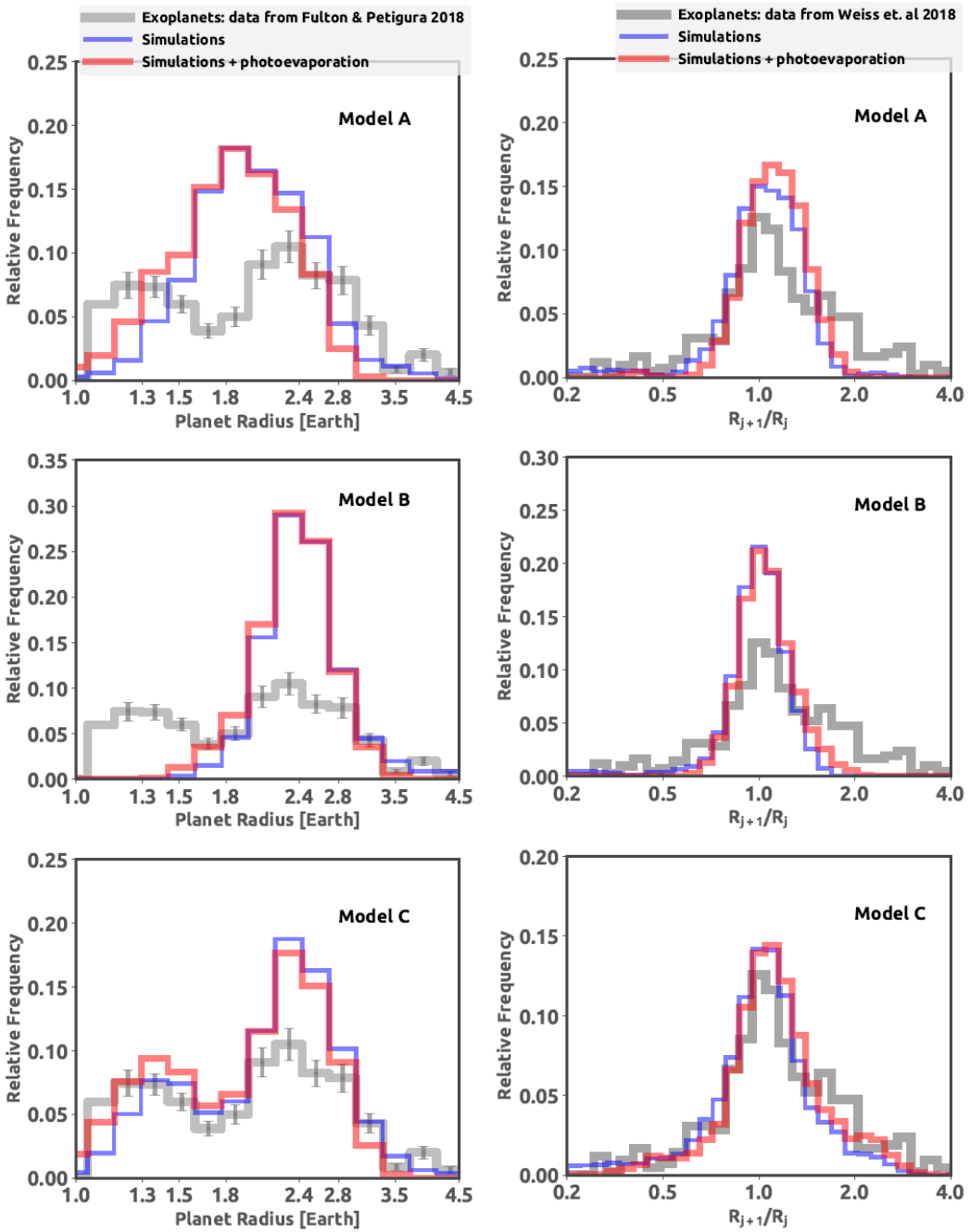

No. 23 **Evidence of a signature of planet formation processes from solar neutrino fluxes**

Masanobu Kunitomo, Tristan Guillot, Gaël Buldgen ★

Solar evolutionary models are thus far unable to reproduce spectroscopic, helioseismic, and neutrino constraints consistently, resulting in the so-called solar modeling problem. In parallel, planet formation models predict that the evolving composition of the protosolar disk and, thus, of the gas accreted by the proto-Sun must have been variable. We show that solar evolutionary models that include a realistic planet formation scenario lead to an increased core metallicity of up to 5%, implying that accurate neutrino flux measurements are sensitive to the initial stages of the formation of the Solar System. Models with homogeneous accretion match neutrino constraints to no better than 2.7σ. In contrast, accretion with a variable composition due to planet formation processes, leading to metal-poor accretion of the last ∼4% of the young Sun's total mass, yields solar models within 1.3σ of all neutrino constraints. We thus demonstrate that in addition to increased opacities at the base of the convective envelope, the formation history of the Solar System constitutes a key element in resolving the current crisis of solar models.

- 太陽ニュートリノの観測的制限を、惑星形成の効果を考えることで説明できるかどうかを議論
- 太陽の進化の計算。全域が対流層になっている初期の段階からの進化を計算する。惑星形成の効果は、円盤からのダストの供給により、重元素が太陽に入ってくる効果として導入。
- 現在の太陽質量の 4% ほどの重元素が、太陽形成の初期に持ち込まれ、中心部まで対流で達することで、中心コア部分の重元素量が増加。その結果、中心コアでの核融合反応で出てくるニュートリノの量に影響が出る。
- 時間依存した重元素の供給を考えることで、太陽ニュートリノの観測により合う進化モデルを作ることができる。

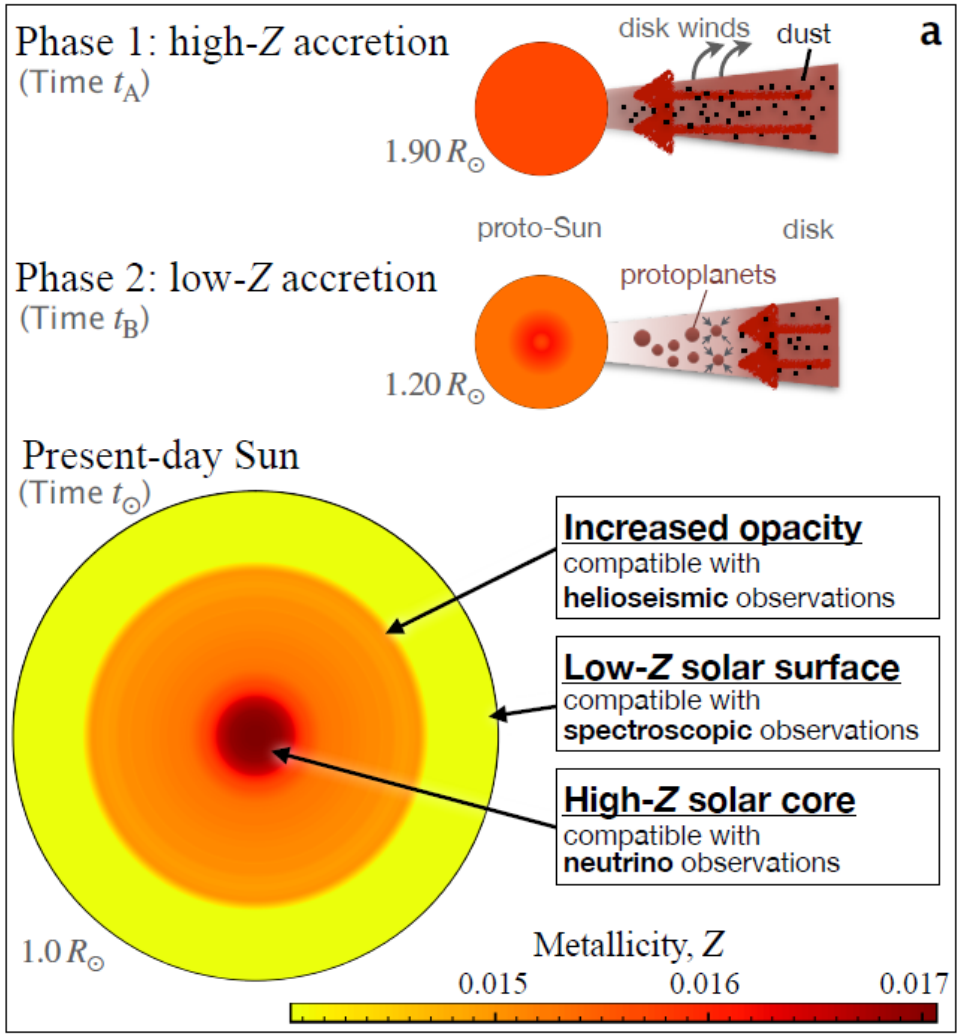

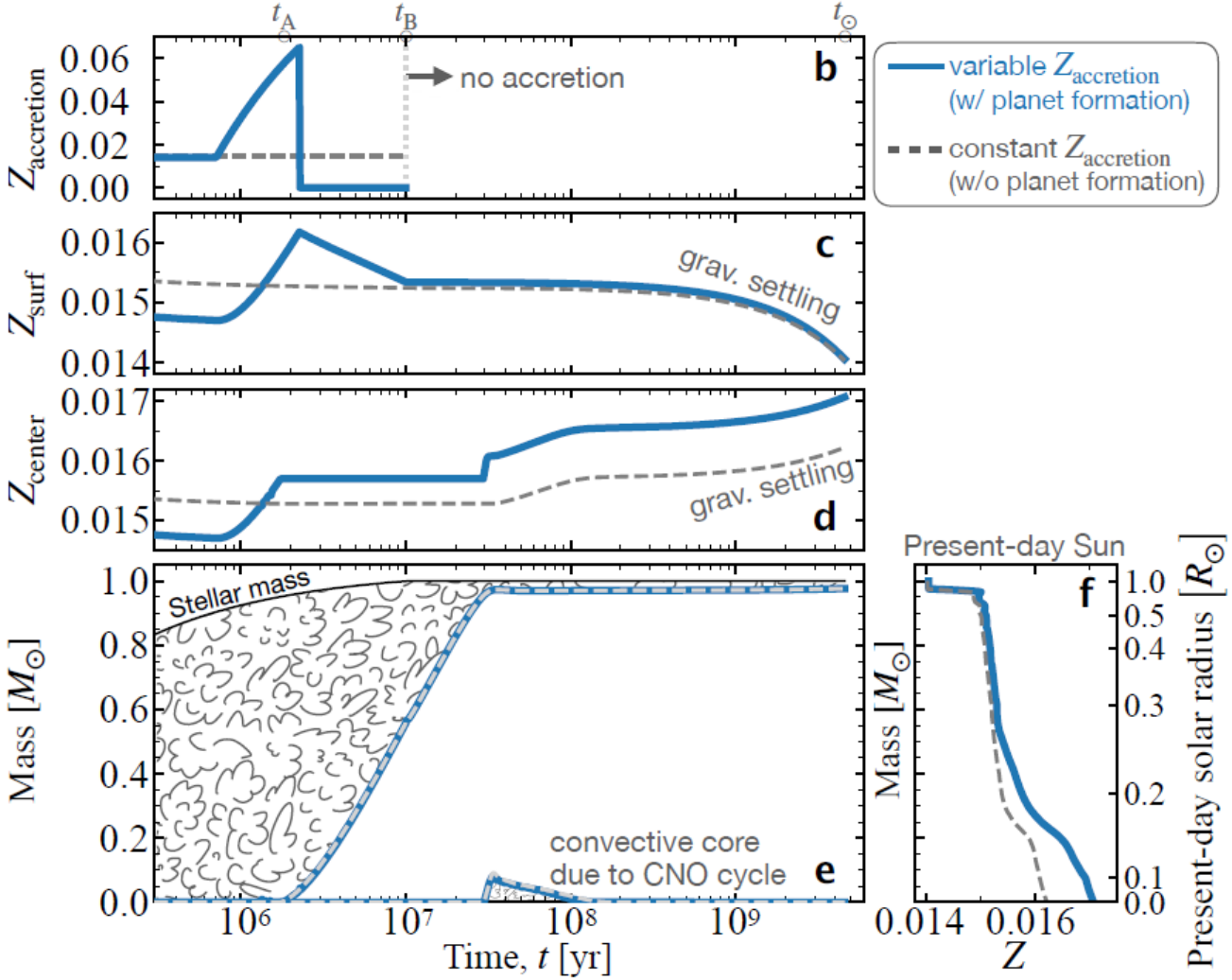

惑星形成：

- 初期にダストがたくさん太陽に降る。この時太陽内部では対流が強い。
- 原始惑星ができると、ダストが無くなるので、重元素の供給が無くなる。

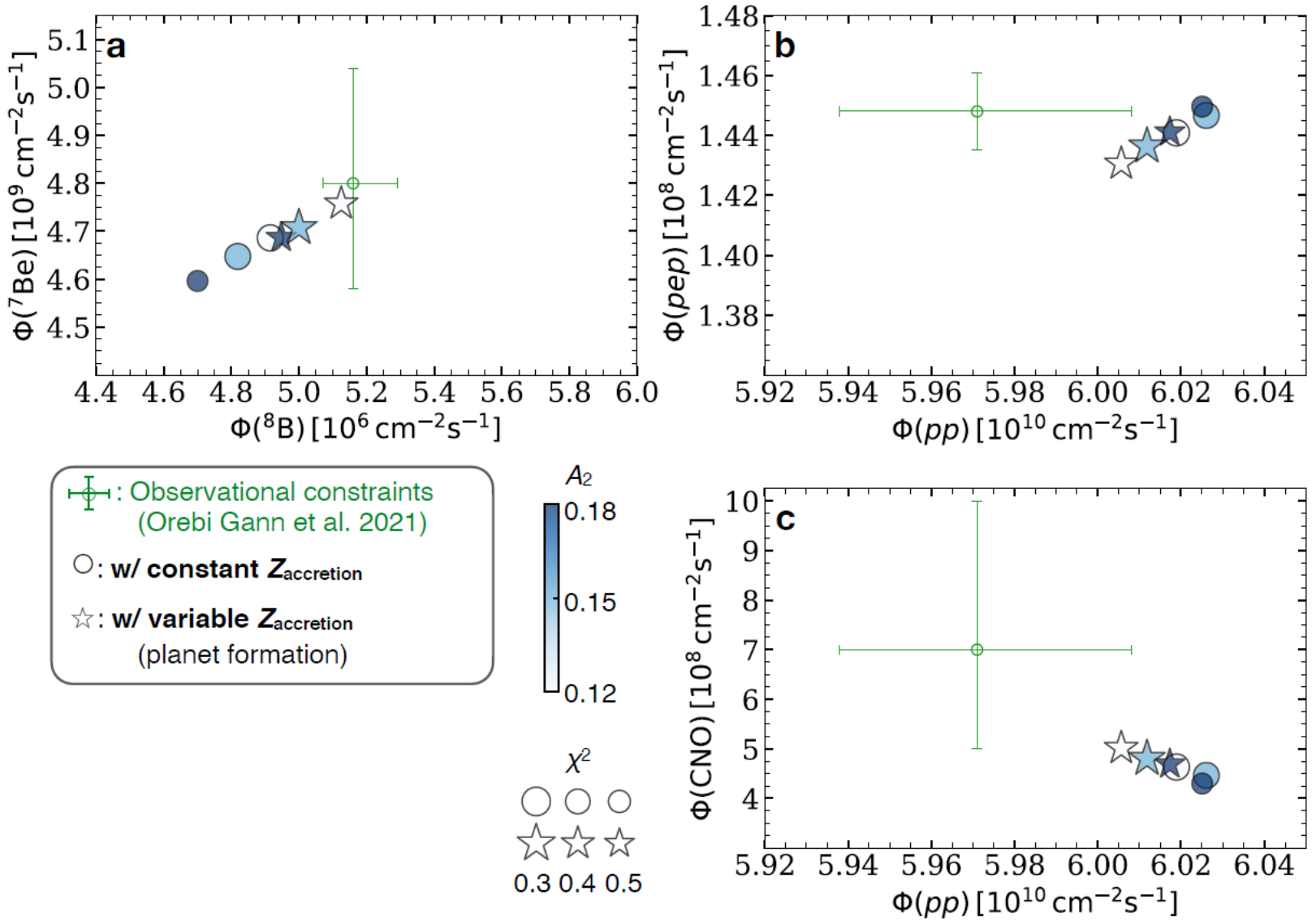

ニュートリノ観測の制限との比較。
ベストフィットは、白抜きの星印。
pep によるニュートリノの制限から、1.3 sigma でしか外れない

No. 15

A HARPS radial velocity search for planets in the Scorpius-Centaurus association. And its combination with the HARPS and SOPHIE young nearby stars (YNS) surveys

Antoine Grandjean, A. -M. Lagrange, N. Meunier, G. Chauvin, S. Borgniet, S. Desidera, F. Galland, F. Kiefer, S. Messina, D. Iglesias, B. Nicholson, B. Pantoja, P. Rubini, E. Sedaghati, M. Sterzik, N. Zicher ★

The Scorpius-Centaurus (Sco-Cen) young and nearby massive star-forming region is particularly well suited for extrasolar planet searches with both direct imaging and radial velocity (RV) techniques. The RV search, however, is challenging, as the stars are faster rotators on average than their older stellar counterparts of similar spectral types. Moreover, the RV time series show strong signatures of stellar variability (spots and faculae) and/or stellar pulsations. Our aim is to search for giant planets (GPs) and brown dwarfs at short orbital distances around star members of the Sco-Cen association. We also aim at using these data together with others available on young stars to estimate the GP occurrence rate for young stars for periods of up to 1000 days. We used the HARPS spectrograph on the 3.6m telescope at the La Silla Observatory to monitor 88 A-F Sco-Cen stars. To improve our statistics and analysis, we combined this survey with two previous surveys that focused on young nearby stars (YNS) to compute companion occurrence rates from a sample of 176 young A-M stars. We report the discovery of a massive hot-Jupiter candidate around HD 145467, together with the discovery of one probable short-period (P $<$ 10 days) brown dwarf around HD 149790. In addition, we confirm the binary nature of eight single-line binaries: HD 108857, HD 108904, HD 111102, HD 114319, HD 121176, HD 126488, HD 126838, and HD 133574. From our sample, we obtain a GP ($m_c \in [1;13] M_{Jup}$) occurrence rate of $0.7^{+1.6}_{-0.2}$ % for periods between 1 and 1000 days and a brown dwarf ($m_c \in [13;80] M_{Jup}$) occurrence rate of $0.6^{+1.4}_{-0.2}$ %, in the same period range. In addition, we report a possible lack of close ($P \in [1;1000] days$) GPs around young F-K stars compared to their older counterparts, with a confidence level of 95%.

- HARPS による、Sco-Cen association の RV サーベイ
- Hot Jupiter candidate 1つ、短周期 Brown dwarf 1つ、single-line binary ８天体でバイナリー的な振る舞い
- 周期 1-1000日の巨大惑星の出現率は 0.7%, brown dwarf は 0.6%
- 若い F-K 型星の周囲には、周期 1-1000日の巨大惑星が、（年齢の進んだ F-K型星に比べて）少ないかもしれない

No. 17

The JCMT BISTRO Survey: A Spiral Magnetic Field in a Hub-Filament Structure, Monoceros R2

Jihye Hwang et al. ★ We present and analyze observations of polarized dust emission at 850 μm towards the central 1 pc × 1 pc hub-filament structure of Monoceros R2 (Mon R2). The data are obtained with SCUBA-2/POL-2 on the James Clerk Maxwell Telescope (JCMT) as part of the BISTRO (B-fields in Star-forming Region Observations) survey. The orientations of the magnetic field follow the spiral structure of Mon R2, which are well-described by an axisymmetric magnetic field model. We estimate the turbulent component of the magnetic field using the angle difference between our observations and the best-fit model of the underlying large-scale mean magnetic field. This estimate is used to calculate the magnetic field strength using the Davis-Chandrasekhar-Fermi method, for which we also obtain the distribution of volume density and velocity dispersion using a column density map derived from *Herschel* data and the $C^{18}O$ (J = 3-2) data taken with HARP on the JCMT, respectively. We make maps of magnetic field strengths and mass-to-flux ratios, finding that magnetic field strengths vary from 0.02 to 3.64 mG with a mean value of 1.0 ± 0.06 mG, and the mean critical mass-to-flux ratio is 0.47 ± 0.02. Additionally, the mean Alfvén Mach number is 0.35 ± 0.01. This suggests that in Mon R2, magnetic fields provide resistance against large-scale gravitational collapse, and magnetic pressure exceeds turbulent pressure. We also investigate the properties of each filament in Mon R2. Most of the filaments are aligned along the magnetic field direction and are magnetically sub-critical.

- JCMT BISTRO による、Mon R2 の 1pc x 1pc の hub-filament の偏光観測
- 磁場の強さは、0.02-3.64 mG の範囲で、平均は 1 mG
- 磁場構造は、Mon R2 のスパイラル構造に沿っている
- Mass-to-flux ratio の平均は 0.47、Alfven Mach number の平均は 0.35
- Mon R2 では、large scale の重力収縮に磁場が対抗しており、磁気圧は乱流圧より大きい

No. 18

A survey for variable young stars with small telescopes: VII – Spot Properties on YSOs in IC5070

Carys Herbert, Dirk Froebrich, Aleks Scholz ★
We present measurements of spot properties on 31 young stellar objects, based on multi-band data from the HOYS (Hunting Outbursting Young Stars) project. On average the analysis for each object is based on 270 data points during 80 days in at least 3 bands. All the young low-mass stars in our sample show periodic photometric variations. We determine spot temperatures and coverage by comparing the measured photometric amplitudes in optical bands with simulated amplitudes based on atmosphere models, including a complete error propagation. 21 objects in our sample feature cool spots, with spot temperatures 500 - 2500 K below the stellar effective temperature ($T_{\rm eff}$), and a coverage of 0.05 - 0.4. Six more have hot spots, with temperatures up to 3000 K above $T_{\rm eff}$ and coverage below 0.15. The remaining four stars have ambiguous solutions or are AA Tau-type contaminants. All of the stars with large spots (i.e. high coverage > 0.1) are relatively cool with $T_{\rm eff} < 4500$ K, which could be a result of having deeper convection zones. Apart from that, spot properties show no significant trends with rotation period, infrared excess, or stellar properties. Most notably, we find hot spots in stars that do not show $K - W2$ infrared excess, indicating the possibility of accretion across an inner disk cavity or the presence of plage.

- 31個の YSO のマルチバンドの測光。80日間、最低でも3バンドで測光。
- 全て周期的な変動を示す。Spot の温度の大きさを求める。
- 21天体は、周囲より 500-2500 K 低いような冷たい spot を持ち、表面の coverage は 0.05-0.4 程度
- 6天体は、周囲より最大で 3000K 高い hot spot を持ち、表面の coverage は 0.15 以下
- 4天体は、うまく spot の性質が求まらなかった
- 大きな spot （coverage で 0.1以上）を持つ天体は、有効温度が 4500K 以下の冷たい天体
- Hot spot を持つ天体で、赤外超過を示さない天体がある。Inner disk cavity を通じた accretion の可能性？

No. 19

Saturation level of turbulence in collapsing gas clouds

Sho Higashi, Hajime Susa, Gen Chiaki ★ We investigate the physical mechanism that decides the saturation level of turbulence in collapsing gas clouds. We perform a suite of high-resolution numerical simulations following the collapse of turbulent gas clouds with various effective polytropic exponents $\gamma_{\rm eff}$, initial Mach numbers $\mathcal{M}_0$, and initial turbulent seeds. Equating the energy injection rate by gravitational contraction and the dissipation rate of turbulence, we obtain an analytic expression of the saturation level of turbulence, and compare it with the numerical results. Consequently, the numerical results are well described by the analytic model, given that the turbulent driving scale in collapsing gas clouds is one-third of Jeans length of collapsing core. These results indicate that the strength of turbulence at the first core formation in the early universe/present-day star-formation process can be estimated solely by $\gamma_{\rm eff}$.

- ガス雲の重力収縮による乱流の saturation level を決めるメカニズムを探るために、（実効的な）ポリトロープ指数、初期のマッハ数、初期の seed 乱流を変えた計算を行なう。
- 重力収縮によるエネルギーの注入と、乱流の散逸率を釣り合わせることで、乱流の saturation level を決める解析的な表式を得た。乱流を起こすスケールが、Jeans 長の 1/3 とすると、数値計算とも良く合う。
- ファーストコアの形成段階での乱流の強さは、実効的なポリトロープ指数で決まる。

No. 22

Filament Formation via Collision-induced Magnetic Reconnection – Formation of a Star Cluster

Shuo Kong, David Whitworth, Rowan J. Smith, Erika T. Hamden ★
A collision-induced magnetic reconnection (CMR) mechanism was recently proposed to explain the formation of a filament in the Orion A molecular cloud. In this mechanism, a collision between two clouds with antiparallel magnetic fields produces a dense filament due to the magnetic tension of the reconnected fields. The filament contains fiber-like sub-structures and is confined by a helical magnetic field. To show whether the dense filament is capable of forming stars, we use the AREPO code with sink particles to model star formation following the formation of the CMR-filament. First, the CMR-filament formation is confirmed with AREPO. Second, the filament is able to form a star cluster after it collapses along its main axis. Compared to the control model without magnetic fields, the CMR model shows two distinctive features. First, the CMR-cluster is confined to a factor of ~ 4 smaller volume. The confinement is due to the combination of the helical field and gravity. Second, the CMR model has a factor of ~ 2 lower star formation rate. The slower star formation is again due to the surface helical field that hinders gas inflow from larger scales. Mass is only supplied to the accreting cluster through streamers.

- 反対向きの磁場を持ったガス雲の衝突によるフィラメント形成（collision-induced magnetic reconnection）
  - フィラメントは、ファイバー状の微細構造を持ち、ヘリカルな磁場に閉じ込められる
- このフィラメントが星を作れるか、フィラメント形成から星形成までを、シンク粒子を入れた AREPO コードを用いて追う
- 磁場無しのモデルと異なる点
  - CMR-cluster はコンパクト、体積で 1/4 ほどの領域に閉じ込められている
  - CMR モデルの星形成率は、磁場無しモデルの半分程度。フィラメント表面付近のヘリカルな磁場により、collapse が阻害される

No. 24

A Multi-Scale Picture of Magnetic Field and Gravity from Large-Scale Filamentary Envelope to Core-Accreting Dust Lanes in the High-Mass Star-Forming Region W51

Patrick M. Koch, Ya-Wen Tang, Paul T. P. Ho, Pei-Ying Hsieh, Jia-Wei Wang, Hsi-Wei Yen, Ana Duarte-Cabral, Nicolas Peretto, Yu-Nung Su

★ We present 230 GHz continuum polarization observations with the Atacama Large Milimeter/Submillimeter Array (ALMA) at a resolution of 0.1 arcseconds (∼ 540 au) in the high-mass star-forming regions W51 e2 and e8. These observations resolve a network of core-connecting dust lanes, marking a departure from earlier coarser more spherical continuum structures. At the same time, the cores do not appear to fragment further. Polarized dust emission is clearly detected. The inferred magnetic field orientations are prevailingly parallel to dust lanes. This key structural feature is analyzed together with the local gravitational vector field. The direction of local gravity is found to typically align with dust lanes. With these findings we derive a stability criterion that defines a maximum magnetic field strength that can be overcome by an observed magnetic field-gravity configuration. Equivalently, this defines a minimum field strength that can stabilize dust lanes against a radial collapse. We find that the detected dust lanes in W51 e2 and e8 are stable, hence possibly making them a fundamental component in the accretion onto central sources, providing support for massive star formation models without the need of large accretion disks. When comparing to coarser resolutions, covering the scales of envelope, global, and local collapse, we find recurring similarities in the magnetic field structures and their corresponding gravitational vector fields. These self-similar structures point at a multi-scale collapse-within-collapse scenario until finally the scale of core-accreting dust lanes is reached where gravity is entraining the magnetic field and aligning it with the dust lanes.

- 大質量星形成領域 W51 e2 と e8 の、ALMA による 230GHz 連続波偏光観測。空間分解能 0.1asec~540au
- コアどうしの間をつなぐ dust lane を空間分解。磁場は dust lane に平行。局所的な重力の方向も、dust lane に平行。
- Dust lane が重力で潰れないような最小の磁場強度を見積もると、W51 e2 と e8 は安定であると考えられる。
- 分解能を落とした解析でも似たような構造
  - collapse が、多重構造で起こっていることを示唆

No. 25

On the underestimation of dust mass in protoplanetary disks: Effects of disk structure and dust properties

Yao Liu, Hendrik Linz, Min Fang, Thomas Henning, Sebastian Wolf, Mario Flock, Giovanni P. Rosotti, Hongchi Wang, Dafa Li ★

The total amount of dust grains in protoplanetary disks is one of the key properties that characterize the potential for planet formation. With (sub-)millimeter flux measurements, literature studies usually derive the dust mass using an analytic form under the assumption of optically thin emission, which may lead to substantial underestimation. In this work, we conduct a parameter study with the goal of investigating the effects of disk structure and dust properties on the underestimation through self-consistent radiative transfer models. Different dust models, scattering modes and approaches for dust settling are considered and compared. The influences of disk substructures, such as rings and crescents, on the mass derivation are investigated as well. The results indicate that the traditional analytic method can underestimate the mass by a factor of a few to hundreds, depending on the optical depth along the line of sight set mainly by the true dust mass, disk size and inclination. As an application, we perform a detailed radiative transfer modeling of the spectral energy distribution of DoAr 33, one of the observed DSHARP disks. When the DSHARP dust opacities are adopted, the most probable dust mass returned from the Bayesian analysis is roughly 7 times higher than the value given by the analytic calculation. Our study demonstrates that estimating disk dust masses from radiative transfer modeling is one solution for alleviating the problem of insufficient mass for planet formation raised in the ALMA era.

- サブミリ波のフラックスから、ダスト質量を求める方法を議論。光学的に薄い仮定から、解析的に質量を求めると、underestimate する。
- 円盤に構造があった場合や、ダストの光学的性質が異なる場合、どの程度の underestimate をするかを、輻射輸送を用いたモデルを用いて調べる。
- 良く用いられる解析的な方法では、数倍から100倍程度の underestimate をする。
- DSHARP の DoAr 33 のデータの場合、7倍程度の間違いになる。

No. 26

The effect of collisional erosion on the composition of Earth-analog planets in Grand Tack models: Implications for the formation of the Earth

Allibert L., Siebert J., Charnoz S., Jacobson S. A., Raymond S. N ★ Impact-induced erosion of the Earth's early crust during accretion of terrestrial bodies can significantly modify the primordial chemical composition of the Bulk Silicate Earth (BSE, that is, the composition of the crust added to the present-day mantle). In particular, it can be particularly efficient in altering the abundances of elements having a strong affinity for silicate melts (i.e. incompatible elements) as the early differentiated crust was preferentially enriched in those. Here, we further develop an erosion model (EROD) to quantify the effects of collisional erosion on the final composition of the BSE. Results are compared to the present-day BSE composition models and constraints on Earth's accretion processes are provided. The evolution of the BSE chemical composition resulting from crustal stripping is computed for entire accretion histories of about 50 Earth analogs in the context of the Grand Tack model. The chosen chemical elements span a wide range of incompatibility degrees. We find that a maximum loss of 40wt% can be expected for the most incompatible lithophile elements such as Rb, Th or U in the BSE when the crust is formed from low partial melting rates. Accordingly, depending on both the exact nature of the crust-forming processes during accretion and the accretion history itself, Refractory Lithophile Elements (RLE) may not be in chondritic relative proportions in the BSE. In that case, current BSE estimates may need to be corrected as a function of the geochemical incompatibility of these elements. Alternatively, if RLE are indeed in chondritic relative proportions in the BSE, accretion scenarios that are efficient in affecting the BSE chemical composition should be questioned.

- Grand Tack モデルの枠組みの中で、初期地球への衝突による融解が、地球の composition 与える影響を調べた。
- Rb, Th, U など、シリケイトの融解物と親和性の高い元素は、最大で 40% ほどの質量が失われる。化学組成の推定のためには、この効果を考える必要がある。

No. 27

Stellar population of the Rosette Nebula and NGC 2244: application of the probabilistic random forest

Koraljka Muzic, Victor Almendros-Abad, Herve Bouy, Karolina Kubiak, Karla Pena Ramirez, Alberto Krone-Martins, Andre Moitinho, Miguel Conceicao ★

(Abridged) In this work, we study the 2.8x2.6 deg2 region in the emblematic Rosette Nebula, centred at the young cluster NGC 2244, with the aim of constructing the most reliable candidate member list to date, determining various structural and kinematic parameters, and learning about the past and the future of the region. Starting from a catalogue containing optical to mid-infrared photometry, as well as positions and proper motions from Gaia EDR3, we apply the Probabilistic Random Forest algorithm and derive membership probability for each source. Based on the list of almost 3000 probable members, of which about a third are concentrated within the radius of 20' from the centre of NGC 2244, we identify various clustered sources and stellar concentrations, and estimate the average distance of 1489+-37 pc (entire region), 1440+-32 pc (NGC 2244) and 1525+-36 pc (NGC 2237). The masses, extinction, and ages are derived by SED fitting, and the internal dynamic is assessed via proper motions relative to the mean proper motion of NGC 2244. NGC 2244 is showing a clear expansion pattern, with an expansion velocity that increases with radius. Its IMF is well represented by two power laws ($dN/dM \propto M^{-\alpha}$), with slopes $\alpha = 1.05$+-0.02 for the mass range 0.2 - 1.5 MSun, and $\alpha = 2.3$+-0.3 for the mass range 1.5 - 20 MSun, in agreement with other star forming regions. The mean age of the region is 2 Myr. We find evidence for the difference in ages between NGC 2244 and the region associated with the molecular cloud, which appears slightly younger. The velocity dispersion of NGC 2244 is well above the virial velocity dispersion derived from the total mass (1000+-70 MSun) and half-mass radius (3.4+-0.2 pc). From the comparison to other clusters and to numerical simulations, we conclude that NGC 2244 may be unbound, and possibly even formed in a super-virial state.

- 若い星団NGC2244 周囲に広がる Rosetta Nebula の 2.8x2.6度の領域を調べ、メンバーの同定や構造・運動の情報を得る。
- 3000個程度のメンバー候補があり、そのうち 1/3 は NGC2244 から 20分以内にあった
- NGC 2244 は広がっていく傾向にあり、速度分散はビリアル速度より大きい。NGC 2244 は、 重力的に束縛されていないものと思われる。

No. 28

Long-term Photometric Study of the Pre-main Sequence Star V1180 Cas

Asen Mutafov, Evgeni Semkov, Stoyanka Peneva, Sunay Ibryamov ★
In this paper results from the optical photometric observations of the pre-main-sequence star V1180 Cas are reported. The star is a young variable associated with the dark cloud Lynds 1340, located at a distance of 600 pc from the Sun in the star forming region in Cassiopeia. V1180 Cas shows a large amplitude variability interpreted as a combination of accretion-induced and extinction-driven effects. Our data from VRI CCD photometric observations of the star are collected from September 2011 to February 2022. During our monitoring, we recorded several brightness dips with large amplitudes of up to 5 mag. (I-band). At the same time, increases in brightness over periods of several weeks have also been recorded. In this paper, we compare the photometric data obtained for V1180 Cas with observations of other low-mass pre-main sequence objects.

- 前期主系列星 V1180 Cas の 10年にわたる測光観測。暗黒星雲 Lynds 1340 にある、若い変光星
- I バンドで 5 等くらい、一瞬暗くなったことが何度かあった。また、それが起こったのは、星が数週間にわたって明るくなっていたときだった。